Clemastine Improves Hypomyelination in Rats with Hypoxic–Ischemic Brain Injury by Reducing Astroglia-Derived IL-1β via Autophagy

Di Xie
Shanghai Jiaotong University School of Medicine Xinhua Hospital Chongming Branch
Lei Niu
Shanghai Jiaotong University School of Medicine Xinhua Hospital Chongming Branch
Chengjin Gao
Shanghai Jiaotong University School of Medicine Xinhua Hospital
Xiaoli Ge
Shanghai Jiaotong University School of Medicine Xinhua Hospital
Yang Wang
Shanghai Jiaotong University School of Medicine Xinhua Hospital
Yajie Zhu
Shanghai Jiaotong University School of Medicine Xinhua Hospital
Jialong Tang
Shanghai Jiaotong University School of Medicine Xinhua Hospital
Aihua Fei (feiaihua@xinhuamed.com.cn)
Shanghai Jiaotong University School of Medicine Xinhua Hospital
Shuming Pan (panpanq123q@163.com)
Shanghai Jiaotong University School of Medicine Xinhua Hospital

Research

Keywords: clemastine, nlrp3, autophagy, astrocyte, hypomyelination

Posted Date: May 13th, 2020

DOI: https://doi.org/10.21203/rs.3.rs-28608/v1

Abstract

Background Cardiac arrest can lead to a poor prognosis of the nervous system. Neuroinflammation plays an important role in hypoxic ischemic brain injury (HIBI). Regulation of inflammation via autophagy might be a suitable therapeutic target in HIBI. This study aims to determine whether clemastine can improve hypomyelination by suppressing the activated astrocytes via autophagy and improving axonal hypomyelination in HIBI.

Methods A bilateral common carotid artery occlusion (BCCAO) rat model that received continuous intraperitoneal injection (1 mg/kg) for 14 days was employed to elaborate the neuroprotection effects of clemastine. interleukin-1β (IL-1β), nod-like receptor protein 3 (NLRP3), histamine H1 receptor, autophagy related protein and OPCs differentiation levels in the corpus callosum were measured. Primary cultured OPCs and co-culture of astrocytes and OPCs were used to explore the link between astrocytes activation and hypomyelination. Data were evaluated by one-way ANOVA with Fisher's protected least significant difference test.

Results Clemastine treatment could reverse hypomyelination and restrain the upregulation of IL-1β and NLRP3 in the corpus callosum of BCCAO rats. Primary cultured OPCs treated with IL-1β showed failed maturation. Expression of LC3Ⅱ/Ⅰdecreased after astrocytic activation. Co-culture of astrocytes and OPCs with oxygen glucose deprivation treatment exhibited NLRP3/1β upregulation and PLP downregulation. Clemastine could downregulate NLRP3/1β and reverse hypomyelination by promoting the autophagy.

Conclusions Clemastine could improve axonal hypomyelination by inhibiting astrocytes activation via promoting the autophagy in BCCAO rats, thus might be a viable strategy to inhibit hypomyelination in the corpus callosum of patients with HIBI.

Background

Cardiac arrest can cause severe neurological damage that can result in a long-term unconscious state, and hypoxic–ischemic brain injury (HIBI) is the main cause of this poor prognosis[1]. The role of white matter injury in HIBI has attracted more attention, axonal hypomyelination is the pathological hallmark of HIBI[2–4].

Neuroinflammation has been widely recognized as a possible pathological factor in HIBI[5, 6] because of its involvement in the secretion of inflammatory factors, such as IL-1β[7]. Our previous study showed that nod-like receptor protein 3 (NLRP3) inflammasome activation lead to excessive expression of IL-1β, resulting in axonal hypomyelination[4, 8]. Astrocytes are crucial regulators of neuroinflammation in the injured central nervous system[9]. It has been confirmed that astrocytes are the predominant source of IL-1β[10]. At present, the involvement of autophagy in the regulation of neuroinflammation has drawn substantial scientific interest[11, 12]. Therefore, the activation of autophagy in astrocytes may reduces IL-1β release and axonal hypomyelination.

Clemastine, a first-generation histamine H1 receptor (HH1R) antagonist, is a promising drug in central nervous system diseases[13]. Our previous study showed clemastine can inhibit neuroinflammation and improve axonal hypomyelination[4]. Whether clemastine improves axonal hypomyelination in HIBI through the regulationof astrocytic autophagy is unclear. Meanwhile, the relationship between astrocyte activation and hypomyelination remains unclear. We hypothesize that clemastine may improve axonal hypomyelination by promoting the LC3B signaling pathway to inhibit NLRP3/ IL-1β signaling pathway in astrocytes. This study aims to investigate the molecular mechanism of clemastine in improving axonal hypomyelination after HIBI and to provide a scientific theoretical basis for therapy in HIBI.

Methods

Animals

200–250 g male Sprague-Dawley (SD) rats were used in this study. For this study, we used the following experimental groups: (1) Several SD rats were sham group.(2) Experimental group performed bilateral common carotid artery ligation (BCCAO) .(3) Several SD rats were intraperitoneally injected with clemastine (1 mg/kg) after BCCAO. The rats were then allowed to raise under normoxic conditions for 0.5, 1, 3, 7, 14, 21, 28 days (d) before being sacrificed. Animal handling and experiments were approved by Institutional Animal Care and Use Committee, Shang hai, China.

Primary Culture of Astrocytes

In brief, cerebral hemispheres were separated from 1-day-old postnatal SD rats (Model Animal Research Center, Xin Hua Hospital, Shanghai Jiao Tong University School of Medicine, License No. SYXK (Shanghai) 2018-0038), the meninges and superficial vessels were carefully removed. The cerebral cortex was harvested and digested with 10 ml 0.125% trypsin containing 600 U DNase (Sigma, St. Louis, MO, USA, Cat. No. D4527) for 15 minutes in 37 °C thermostatic water bath. After this, 10 ml of Dulbecco's modified Eagle's medium-F12 nutrient mixture (DMEM-F12) (Invitrogen Life Technologies Corporation, Carlsbad, CA, USA; Cat. No. 31330-038) containing 10% fetal bovine serum (FBS) (Invitrogen Life Technologies Corporation; Cat. No. 10099-141) was added. The tissue was then triturated several times with a 5 ml pipette. The un-dissociated tissue clumps were allowed to settle for one to two minutes. Subsequently, the supernatant was collected and passed through a 70 μm cell strainer to remove the remaining small clumps of tissue; the cell suspension was then centrifuged at 1,500 rpm for five minutes. The supernatant was discarded and the cell pellet was resuspended in 10 ml of DMEM-F12 supplemented with 10% FBS. The resuspended cells were seeded into poly-L-lysine-coated 75 cm2 flasks at a density of 250,000 cells/ml and cultured at 37 °C in humidified 5% CO2/95% air. The medium was changed after 24 h and then replaced every three to four days. After 10 days, the bottom of the flask showed a confluency of cells with mixed glia, including mainly microglia/oligodendrocytes. The mixed cells were cultured for 10 days at 37℃ and 5% CO_2 before shaking at 180 revolutions per minute (rpm) and 37℃ for 1 h to remove microglia cells and oligodendrocytes. After incubation in a humidified

atmosphere of 95% air and 5% CO2 at 37 °C for 24 h, the cells were subjected to different treatments. The astrocytes cultures with above 90% purity were used in this study.

Treatment of Astrocytes Culture

The purified astrocytes were cultured for 1 d at 5% CO_2 and 95% air at 37℃, the cells were subjected to different treatments. To study whether clemastine would affect astrocytes release of inflammatory mediators and autophagy, astrocytes were treated with (Clemastine group) or without (oxygen glucose deprivation, OGD group) 20 ng/ml clemastine for 1 h at 3% oxygen, 5% CO_2 and 92% nitrogen at 37 °C. Control group with equal volume of PBS, Clemastine group were treated with 20 ng/ml clemastine.

Primary Culture of OPCs

The mixed culture is the same as the astrocytes. The mixed cells were cultured for 10 days at 37 °C and 5% CO_2 before shaking at 180 revolutions per minute (rpm) and 37 °C for 1 h to remove microglia cells. The medium was then replaced with fresh DMEM/FBS, and the cultured cells were again shaken at 250 rpm and 37 °C for 20 h to harvest OPCs, followed by incubating on a 10 cm Petri dish for 60 minutes (min) at 37 °C to remove contaminating astrocytes and microglia. Purified OPCs were plated on Poly-D-lysine (PDL) or laminin-coated coverslips and cultured in oligodendrocyte precursor cell medium (OPCM) (Sciencell Research Labortories, USA, No.1601) at 5% CO_2 and 95% air at 37 °C. The OPCs cultures with above 90% purity were used in this study.

Treatment of OPCs Culture

To examine the effects of IL-1β on the differentiated OPCs. The cells were subdivided into the Control group (0.01M PBS); 30 ng/mL IL-1β group; 30 ng/mL IL-1β + 20 ng/mL IL-1 receptor antagonist (IL-1Ra) group; 20 ng/mL IL-1Ra group. The OPCs were cultured in oligodendrocyte precursor cell differentiation culture medium (OPCDM) (Sciencell Research Labortories, USA, No.1631) for 7 d at 5% CO_2 and 95% air at 37 °C.

Co-culture experiment with astrocytes and OPCs

The purified astrocytes were plated on tissue culture inserts for 6-well plates (0.4 μm, Millipore, Cat. No. MCHT06H48) at a density of 1×10^6 cells. The astrocytes were incubated for 1 h in the presence or absence of clemastine (20 ng/mL) or 3-MA (a specific autophagy inhibitor, Topscience Co., Ltd, 5 mM). In order to minimize OPCs damage due to pretreatment of OGD challenge, we have chosen to treat the target drugs (clemastine and 3-MA) before OGD challenge. Each tissue culture insert was placed on the

OPCs in 6-well plates. Co-culture system were treated for 1 h at 3% oxygen, 5% CO_2 and 92% nitrogen at 37 °C, then, cultured in OPCDM at 5% CO_2 and 95% air at 37 °C.

Treatment of Co-culture

To explore whether clemastine would affect OPCs differentiation via autophagy, The co-culture cells were subdivided into Control group, OGD group, OGD + clemastine, OGD + clemastine + 3-MA group.

Western Blot

Proteins were extracted from the corpus callosum or from primary cell culture using a protein extraction kit (Pierce Biotechnology Inc, IL) according to the manufacturer's protocol. Protein concentrations were determined by the Bradford method using bovine serum albumin (BSA) (Sigma-Aldrich, St Louis, MO) as a standard. Samples of supernatants containing 50 µg of protein were heated to 95 °C for 10 min and were separated by sodium dodecyl sulfate–polyacrylamide gel electrophoresis in 10% gel in a Mini-Protein 3 apparatus (Bio-Rad Laboratories, Hercules, CA). Protein bands were electroblotted onto 0.45 lm polyvinylindene difluoride membranes (BioRad) at 1.5 mA/cm2 of membrane for 1 h in Towbin buffer, pH 8.3, to which 20% (volume/volume (v/v)) methanol had been added. After transfer, the membranes were blocked with QuickBlock™ Blocking Buffer (Cat. P0231, Beyotime, China) for 1 h, then incubated with the primary antibodies according to the manufacturer's recommendations. The primary antibodies used were as follows: IL-1β (Rabbit polyclonal IgG 1:1,000), Histamine H1 Receptor (HH1R) (Rabbit polyclonal IgG 1:1,000), 2',3'-cyclicnucleotide 3'-phosphodiesterase (CNPase) (Rabbit polyclonal IgG 1:1,000), Olig2 (Rabbit polyclonal IgG 1:1,000), Nod-like receptor protein 3 (NLRP3) (Rabbit polyclonal IgG 1:1,000) [all from Bioworld Technology, Inc. Cat. No. BS6067, BS2733, BS3461, BS90984, BS90948], PLP (rabbit polyclonal IgG 1:1000) (Sigma; Cat. No. SAB1410977), Nkx2.2 (mouse monoclonal IgG 1:1,000) (Santa Cruz; Cat. No. sc-398951), p62 (Rabbit polyclonal IgG 1:1,000), Beclin-1 (Rabbit polyclonal IgG 1:1,000), LC3B (Rabbit polyclonal IgG 1:1,000), VCAM-1 (Rabbit polyclonal IgG 1:1,000), β-actin (Rabbit polyclonal IgG 1:1,000) [all from Cell Signaling Technology, Cat. No. #23214, #3495, #3868, #14694, #8457]. After three washes with TBST, the membranes were incubated with the horseradish peroxidase (HRP)-conjugated secondary antibodies (Cell Signaling Technology; Cat. No. 7074 (anti-rabbit IgG), 7076 (anti-mouse IgG)) for 1 h. The immunoblots were developed using the enhanced chemiluminescence detection system (Pierce Biotechnology Inc, Rockford, IL). Blots were stripped with stripping buffer (Cat. P0025N, Beyotime, China) and hybridized with total kinases or β-actin. The signal intensity of these proteins levels relative to control was measured with Quantity One Software, version 4.4.1 (BioRad Laboratories).

Double Immunofluorescence

The Cat. No. of antibody is the same as that of western blot and it is listed separately if there are differences. Immunofluorescence intensity is expressed by mean fluorescence intensity via Image J. The sections from control and BCCAO rats (in each group at 1, 3, 7, 14 and 21 days) were divided into four groups. The sections in group I from control and BCCAO rats at 1, 3 and 7days were then incubated with antibodies directed against anti-IL-1β (Rabbit polyclonal IgG 1:500) or anti-Histamine H1 Receptor (Rabbit polyclonal IgG 1:200) or NLRP3 (Rabbit polyclonal IgG 1:200) and GFAP (Mouse monoclonal IgG 1:100) (Bioworld Technology, Cat. No. MB9017). The sections in group II from control and BCCAO rats at 14 and 21 days were incubated with Olig2 (Rabbit polyclonal IgG 1:200) and NG2 (mouse monoclonal IgG 1:100) .

The sections in group Ⅲ from control and BCCAO rats at 1 day were incubated with LC3B (Rabbit polyclonal IgG 1:1,000). The sections in group Ⅳfrom control and BCCAO rats at 21 day were incubated with CNPase (mouse monoclonal IgG 1:1,000) (Chemicon International; Cat.No. NE1020) or PLP (rabbit polyclonal IgG 1:1000). The incubation for all groups was carried out at 4 °C overnight. On the following day, the sections were washed and incubated with a secondary antibody: Alexa Fluor 555 goat anti-rabbit IgG (1:100, Life, Cat. No. A21428) or Alexa Fluor 555 goat anti-mouse IgG (1:100, Life, Cat. No. A21424) or FITC goat anti-mouse IgG (Bioworld Technology, Inc. Cat. No. BS50950) at room temperature for 1 h. The ratio of NG2/Olig2-positive oligodendrocytes was calculated and averaged. The ratio of NG2/Olig2-positive oligodendrocytes in the corpus callosum was calculated by counting four randomly selected microscopic fields in sections obtained from each rat at 40 × objective by a blinded observer.

For astrocytes cultured, the cells were treated with oxygen glucose deprivation (OGD) and OGD + clemastine for 1 h, respectively (for IL-1β or HH1R and NLRP3 detection), and then fixed in 4% paraformaldehyde for 30 min, blocked in 1% BSA for 30 min and incubated with primary antibodies overnight at 4 °C. The cells were divided into two groups. The cells in group I were carried out by using primary antibodies directed against anti-IL-1β (Rabbit polyclonal IgG 1:500) or anti-Histamine H1 Receptor (Rabbit polyclonal IgG 1:200) or NLRP3 (Rabbit polyclonal IgG 1:200) and GFAP (Mouse monoclonal IgG 1:100) for astrocytes cultured for 1 h.The cells in group II were carried out by using primary antibodies directed against anti-LC3B (Rabbit polyclonal IgG 1:200) and GFAP (Mouse monoclonal IgG 1:100) for astrocytes cultured for 1 h. The cells were then incubated with Alexa Fluor 555 goat-anti-rabbit secondary antibody (1:100, Life, Cat. No. A21428) and FITC goat anti-mouse IgG (Bioworld Technology, Inc. Cat. No. BS50950) for 1 h. Finally, the cells were counterstained with DAPI and examined under a fluorescence microscope (Olympus System Microscope Model BX53, Olympus Company Pte, Tokyo, Japan).

For cultured OPCs, the cells were treated with IL-1β or IL-1Ra and IL-1β + IL-1Ra, respectively, and the same volume of PBS as control for 7 d (for NG2 and PLP detection), then fixed in 4% paraformaldehyde for 30 min, blocked in 1% BSA for 30 min and incubated with primary antibodies overnight at 4°C. Immunofluorescence labeling was carried out by using primary antibodies directed against NG2 (Mouse monoclonal IgG 1:1,000) and PLP (Rabbit polyclonal IgG 1:1000) or VCAM1 (Rabbit polyclonal IgG 1:1000) and PLP (Mouse monoclonal IgG 1:1,000) (Sigma; Cat. No. SAB1404221), respectively. The cells

were then incubated with Alexa Fluor 555 goat anti-rabbit IgG (1:100, Life, Cat. No. A21428) or Alexa Fluor 555 goat anti-mouse IgG (1:100, Life, Cat. No. A21424) or FITC goat anti-mouse IgG (Bioworld Technology, Inc. Cat. No. BS50950) for 1 h. Finally, the cells were counterstained with DAPI and examined under a fluorescence microscope (Olympus System Microscope Model BX53, Olympus Company Pte, Tokyo, Japan). Quantitative analysis of the ratio of NG2, and PLP positive cells was carried out through counting four randomly selected microscopic fields at 40 × objective by a blinded observer. The percentage of cells with positive expression for the respective antibodies was calculated and averaged. Each experiment was done in triplicate.

Electron Microscopy

The BCCAO rats, BCCAO + clemastine rats at 1, 28 days and their corresponding control rats were perfused with a mixed aldehyde fixative composed of 2% paraformaldehyde and 3% glutaraldehyde in 0.1M phosphate buffer, pH 7.2. After perfusion, the brain was removed and coronal slices (approximately 1 mm thick) were cut. Blocks of corpus callosum were trimmed from these slices.Vibratome sections (Model 3000TM, The Vibratome Company, St. Louis, MO) of 80–100 mm thickness were prepared from these blocks and rinsed overnight in 0.1M phosphate buffer. They were then post-fixed for 2 h in 1% osmium tetraoxide, dehydrated, and embedded in Araldite mixture. Ultrathin sections were cut and viewed in a Philips CM 120 electron microscope (FEI Company, Hillsboro, OR). Four non-overlapping regions of the medial corpusallosum from each animal were photographed at two different magnifications. The diameter of each axon as well as that of axon plus its associated myelin sheath was measured by using Image J software (SummaSketch III Summagraphics, Seattle, WA). The g-ratio was calculated per axon as axon diameter to total axonal fiber diameter, the transmission electron microscope was finally used to detect the autophagosomes in astrocytes.[it is equivalent to axon area/(axon + myelin sheath area)] by a researcher blind to control/BCCAO/clemastine injection group and compared among groups with one-way ANOVA ($\alpha = 0.05$, two-tailed; $n = 3$ per group).

Statistical Analysis

All data were evaluated by the SPSS13.0 statistical software (IBM, Armonk, NY). Different statistical methods were applied according to different types of data. The distribution values were expressed as mean ± SD. Four-group univariate-factor measurement data were analyzed by one-way ANOVA if the data were homogeneity of variance; otherwise, they were analyzed by Welch ANOVA. Multiple comparisons were analyzed by the least significant difference (LSD) method if the data were homogeneity of variance; otherwise they were analyzed by Dunnett's T3 method. The criterion for statistical significance was set at $P < 0.05$.

Results

1. Determining IL-1β, NLRP3, and HH1R protein expression levels in the corpus callosum by double labeling and Western blot analysis

In the corpus callosum of the control rats, the interleukin-1beta (IL-1β) and NLRP3 expression levels were specifically detected in sporadic cells and confirmed to be astrocytes by double labeling with GFAP staining (Figs. 1A–1I and 1K–1S). At 1 day following bilateral common carotid artery occlusion (BCCAO), the IL-1β and NLRP3 immunoreactivities were induced in astrocytes (Figs. 1D–1F and 1N–1P) when compared with that of the controls (Figs. 1A–1C and 1K–1M). However, clemastine reversed these changes (Figs. 1G–1I and 1Q–1S). The excessive expression levels of IL-1β and NLRP3 decreased after treatment with clemastine (Figs. 1J and 1T, respectively). The expression of HH1R was localized in the astrocytes as confirmed by double immunofluorescence showing colocalization of GFAP staining (Figs. 2A–2I). At 1 day following BCCAO, the HH1R immunoreactivity was markedly enhanced in the soma of astrocytes (Figs. 2D–2F) compared with that of the control (Figs. 2A–2C). However, clemastine caused no effect on its expression (Figs. 2G–2I and 2J). The immunoreactive bands of IL-1β and NLRP3 protein levels, which appeared at approximately 17 and 62 kDa, respectively (Fig. 1U), increased significantly (*$P < 0.05$) in optical density at 1, 3, and 7 days after BCCAO compared with that of the controls. However, clemastine could reverse this phenomenon (Figs. 1V and 1W). The immunoreactive bands of HH1R protein levels, which appeared at approximately 70 kDa (Fig. 2K), increased significantly (*$P < 0.05$) in optical density at 1 day after BCCAO compared with that of the controls; clemastine showed no effect on the expression of HH1R (Fig. 2L).

2. p62, LC3B and Beclin-1 protein expression levels in the corpus callosum

In the corpus callosum of the control rats, the LC3B expression levels were detected (Figs. 3A–3C). At 1 day following bilateral common carotid artery occlusion (BCCAO), the LC3B immunoreactivities were decreased in corpus callosum (Figs. 3B) when compared with that of the controls (Figs. 3A). However, clemastine reversed these changes (Figs. 3C). The ratio of DAPI/LC3B increased after treatment with clemastine (Figs. 3D). The immunoreactive bands of p62, LC3B and Beclin-1 protein levels, which appeared at approximately 62, 17 and 65 kDa, respectively (Fig. 3E). p62 increased and LC3B, Beclin-1 decreased significantly (*$P < 0.05$) in optical density at 0.5, 1, and 3 days after BCCAO compared with that of the controls. However, clemastine could reverse this phenomenon (Figs. 3J-L). Transmission electron microscopy of brain revealed that astrocytes after BCCAO presented less cytoplasmic vacuolization than that in contro at l day. The vacuoles were filled with amorphous or electron-dense material and were surrounded by a single or a double membrane(Fig. 3M and 3N). clemastine could reverse this phenomenon(Fig. 3O). In summary, clemastine promoted autophagy in astrocytes.

3. Expression of Olig2 and Nkx2.2 in the corpus callosum at 14, 21, and 28 days

To observe the maturation of OPCs, we used transcription molecules of OPCs, such as oligodendrocyte transcription factor 2 (Olig2), Nkx2.2 and neural/glial antigen 2 (NG2), to detect the ratio of OPCs in the corpus callosum. The ratio of NG2/Olig2-positive OPCs remarkably decreased in the corpus callosum at 14 day after BCCAO in comparison with that of the corresponding controls; however, clemastine showed no effect on the expression of NG2 and upregulated the expression of Olig2 at 14 and 21days (Figs. 4A–4H; *P< 0.05). The immunoreactive bands of Olig2 and Nkx2.2 proteins, which appeared at approximately 32 and 34 kDa, respectively (Fig. 4I), decreased significantly at 21 days after BCCAO compared with that of the controls. Olig2 protein increased significantly at 14 day and Nkx2.2 protein increased at 21 day after treatment with clemastine compared with that of BCCAO (Fig. 4J and 4K; *P< 0.05).

4. PLP, CNPase and VCAM1 protein expression levels in the corpus callosum

Proteolipid protein (PLP) and 2′,3′-cyclic nucleotide-3′-phosphodiesterase (CNPase) are useful and specific markers for mature myelin sheath in the central nervous system (CNS). Immunostaining showed that PLP and CNPase protein expression levels decreased in the corpus callosum at 21 days after BCCAO compared with their age-matched littermates (Figs. 5A–4C and 5D–4F); however, clemastine could reverse this phenomenon (Figs. 5G and 5H). The immunoreactive bands of PLP and CNPase protein levels decreased significantly in optical density in the corpus callosum at 7, 14, and 28 days after BCCAO (Fig. 5I). However, clemastine could reverse this phenomenon at 28 days (Figs. 5J and 5K). Vascular cell adhesion molecule 1 (VCAM1) protein decreased significantly at 7 and 14 days after treatment with clemastine compared with that of BCCAO, clemastine could reverse this phenomenon at 7 days.(Fig. 5L; *P< 0.05). These findings indicated that BCCAO can cause hypomyelination, whereas clemastine can alleviate hypomyelination in CNS. From the electron microscopy (EM) observation, the packing density of myelinated axons remarkably reduced as manifested by the loosely organized fibers in the corpus callosum at 28 days after BCCAO (Fig. 5N) compared with that of the corresponding controls (Fig. 5M). however, clemastine alleviated this condition (Fig. 5O). The g-ratios were measured by determining the axon diameter/fiber diameter of myelinated axons to analyze the structural deficits quantitatively. The averaged g-ratio in 28-day control rats reached 0.64. The value significantly increased to 0.75 in rats after BCCAO. After the intervention by clemastine, the averaged g-ratio totaled 0.69, indicating that clemastine reversed the reduced myelin thickness in BCCAO rats (Figs. 5M–5O and 5P). Therefore, the EM results demonstrated the few myelinated fibers and thin myelin sheaths in the corpus callosum at 28 days after BCCAO. On the contrary, clemastine could promote myelin formation in the myelinated fibers.

5. IL-1β could inhibit the maturation of OPCs in vitro

Immunofluorescence and Western blot were employed to explore the effect of IL-1β on the maturation of OPCs and measure the maturation of the same number of primary OPCs in the differentiation medium for 7 days after administration with IL-1β, IL-1β + IL-1 receptor antagonist (IL-1Ra), and an equal volume of phosphate-buffered saline (PBS) as control. The percentage of NG-positive OPCs at 7 days following the administration of IL-1β was considerably higher than that in the corresponding controls and PLP-positive oligodendrocytes was lower (Figs. 6A and 6B). However, IL-1Ra could revert the inhibition of IL-1β on the maturation of primary OPCs (Fig. 6C, 6G and 6H). The VCAM1 at 7days following the administration of IL-1β was decreased (Figs. 6E) when compared with that of the controls (Figs. 6D). However, IL-1Ra reversed these changes (Figs. 6F and 6I). The protein expression levels of PLP, CNPase and VCAM1 considerably decreased at 7 days after the administration of IL-1β compared with that of the controls (Figs. 6J–6M). However, the administration of IL-1Ra could revert the expression of the abovementioned proteins (Figs. 6J–6M). Thus, in vitro data showed that IL-1β could inhibit the maturation of primary OPCs.

6. Clemastine inhibits astrocytic activation in vitro

Culture of astrocytes was established to explore the effect of clemastine on the activation of astrocytes in vitro. Double immunofluorescence showed higher expression levels of IL-1β and NLPR3 characterized at 1 h after OGD (Figs. 7D–7F and 7M–7O, respectively) in comparison with that of the controls (Figs. 7A–7C and 7J–7L). On the contrary, clemastine could remarkably reduce the expression levels of IL-1β and NLRP3 (Figs. 7G–7I and 7P–7T). The protein expression levels of IL-1β and NLRP3 considerably increased at 1 h after administration of OGD compared with that of the controls (Figs. 8K–8M). The administration of clemastine could revert the expression levels of IL-1β and NLRP3 proteins (Figs. 8K–8M). Thus, in vitro data showed that clemastine could inhibit the activation of astrocytes.

7. Clemastine caused no effect on the expression of HH1R in astrocytes

Double immunofluorescence was performed to explore the effect of clemastine on the expression of HH1R in astrocytes in vitro. In addition, a higher expression of HH1R was observed at 1 h after OGD (Figs. 8D–8F) compared with that of the controls (Figs. 8A–8C). Moreover, clemastine did not affect the expression of HH1R (Figs. 8G–8J), which was similar to the results of Western blot (Figs. 8K and 8N). Thus, the in vitro data showed that clemastine does not influence the expression of HH1R in astrocytes.

8. Clemastine improves autophagy of astrocytes in vitro

Double immunofluorescence was performed to explore the effect of clemastine on the autophagy in astrocytes in vitro. In addition, a lower expression of LC3B was observed at 1 h after OGD (Figs. 9D–9F) compared with that of the controls (Figs. 9A–9C). Clemastine could remarkably improve the expression levels of LC3B (Figs. 9G–9I), which was similar to the results of western blot (Figs. 9L). The immunoreactive bands of LC3B and p62 protein levels, which appeared at approximately 17 and 62 kDa, respectively (Fig. 9J). p62 increased and LC3B decreased significantly (*$P < 0.05$) in optical density at 1 h after OGD compared with that of the controls. However, clemastine could reverse this phenomenon (Figs. 9K and 9L). Thus, the in vitro data showed that clemastine improves autophagy of astrocytes in vitro.

9. Clemastine improves axonal hypomyelination via activation of autophagy in astrocytes

We hypothesized that clemastine improves axonal hypomyelination via activation of autophagy in astrocytes. To ascertain this assumption, the protein expression levels of NLRP3 and IL-1β were measured by western blot in astrocytes at 1 h (Figs. 9M). The protein expression levels of NLRP3 and IL-1β were remarkably upregulated at 1 h after treatment with OGD compared with that of the controls. On the contrary, clemastine could improve the high expression levels of NLRP3 and IL-1β proteins. The effection was weakened after adding additional 3-MA (a specific autophagy inhibitor;Figs. 9N and 9O). Co-culture of astrocytes with OPCs was established to examine the link between hypomyelination and the autophagy of astrocytes. The protein expression levels of PLP and VCAM1 were remarkably downregulated at 3 days after OGD compared with that of the controls (Fig. 9P). However, clemastine could upregulate the expression levels of PLP and VCAM1 proteins induced by OGD. When additional 3-MA was added, the expression of PLP and VCAM1 was downregulated compared with the OGD + clemastine group(Fig. 9P-R). Thus, the in vitro data substantiated that clemastine could improve axonal hypomyelination by activation of autophagy in astrocytes.

Discussion

Neuroinflammation plays an important role in the pathogenesis of HIBI[14]. Activated astrocytes elicit neuroinflammation and release inflammatory cytokines such as IL-1β [15], which leads to axonal hypomyelination [16]. Recent studies showe that NLRP3 considers to be crucial for secretion of IL-1β [17, 18]. The results showed a remarkable increase in the levels of IL-1β and NLRP3 in BCCAO rats up to 1 day. Double immunofluorescence staining has shown that NLRP3 and IL-1β expression levels which are localized in the astroglia activated after ischemia–hypoxia. Our previous research found that HH1R is associated with neuroinflammation[4]. The results showed that HH1R exists in the astrocytes and the expression levels of IL-1β and NLRP3 were decreased by clemastine (H1 receptor antagonist), but the expression of HH1R was unaffected and localized in the astrocytes. Autophagy is a lysosome-dependent, homeostatic process, in which organelles and proteins are degraded and recycled into energy[19]. inhibition of autophagy may enhance microglia activity, including secretion of cytokines such as Il-1β in

vitro[20]. Autophagy is a highly dynamic, multi-step process. Like other cellular pathways, it can be modulated at several steps. The amount of lipidated LC3 [LC3-II] could reflect the inability of turnover to keep pace with increased autophagosome formation[21]. Then, the conjugation of LC3 to single-membrane phagosomes, a process that promotes autophagic flow and result in the recruitment of the Beclin-1[22]. P62 is an autophagy receptor that links ubiquitinated proteins to LC3, which accumulates in cells when macroautophagy is inhibited[23, 24]. The present results showed that the LC3Ⅱ/Ⅰ and Beclin-1 remarkably decreased in the corpus callosum at 1 days after ischemia–hypoxia. clemastine increased the expression of LC3Ⅱ/Ⅰand Beclin-1 at 1 days. The trend of p62 is opposite to LC3Ⅱ/Ⅰand Beclin-1. It is suggested that autophagy is inhibited after ischemia–hypoxia, and clemastine can improve autophagy flux. Electron microscope is best used in combination with other methods to ensure the complex and holistic approach that is becoming increasingly necessary for further progress in autophagy research.The present data suggested that the number of autophagy bodie downregulated in the astrocytes at 1 days after ischemia–hypoxia, clemastine reversed this phenomenon. In summary, indicating that clemastine may also promote the autophagy. NG2 is a type-1 membrane protein, which is expressed by OPCs[25]. OPCs gradually differentiated into mature oligodendrocytes labeled CNPase or PLP under the action of differentiation promoting transcription factors[26, 27]. The maturation of OPCs plays an important role in the myelination of targeting axons. Several transcription factors are involved in the maturation of OPCs, such as Olig2, Nkx2.2, which promotes the maturation of OPCs[28, 29]. Rcent research has suggested that VCAM1 knockout mice exhibit reduced myelin thickness, VCAM1 contributes to the initiation of myelination[30]. The present results showed that the ratio of NG2/Olig2-positive OPCs remarkably decreased in the corpus callosum at 14 days after ischemia–hypoxia. clemastine increased the expression of Olig2 and Nkx2.2 at 21days. The present data suggested that the expression levels of PLP and CNPase were downregulated in the corpus callosum at 21 days and the proportion of myelinated axons and thin myelin sheath decreased at 28 days after ischemia–hypoxia. These results indicated that the myelin sheath formation was disrupted, clemastine reversed this phenomenon. Indicating that clemastine may also promote the maturation of OPCs by improving forward transcription factors. We observed that clemastine can inhibit the secretion of IL-1β and autophagic flux, promote the differentiation of OPCs and improve axonal hypomyelination. However, the mechanism remains unknown. The IL-1β is a key mediator of the complex inflammatory response, IL-1β resulted in attenuated loss of mature oligodendrocytes[31]. Interleukin-1 receptor antagonist (IL-1Ra), as well as IL-1R1 knockout, improved remyelination[32]. In vitro results showed that IL-1β administration delayed the development of oligodendrocytes, as evidenced by the decreased expression levels of PLP, CNPase, VCAM1 and as opposed to the increased expression levels of NG2. IL-1Ra, when administered in vitro, can revert this situation. Activated astrocytes can release IL-1β, which leads to tissue damage[33]. The present data showed that the expression levels of NLRP3, IL-1β and HH1R were upregulated at 1 h after OGD. Clemastine can reverse this phenomenon, indicating that clemastine can inhibit the activation of astrocytes. However, the mechanism remains unknown. Autophagy has been shown to regulate astrocyte activation, is critical for maintaining astrocytic functions[34, 35]. We hypothesized that clemastine inhibited IL-1β secretion by promoting autophagy. The present study revealed that the expression levels of p62 increased after hypoxia. Furthermore, clemastine could reduce the excessive expression levels of

p62, the trend of LC3Ⅱ/Ⅰ is opposite to p62. The expression levels of NLRP3 and IL-1β increased after hypoxia, clemastine had anti-inflammatory effect. When 3-MA, a autophagy inhibitor, is added, the effect weakened. Suggesting that clemastine featured an anti-inflammatory effect via autophagy. Co-culture of astrocytes with OPCs was established to verify the link between axonal hypomyelination and activation of astrocytes. The present research showed that the expression levels of PLP and VCAM1 remarkably decreased and the expression levels of VCAM1 and PLP improved after clemastine treatment of the OPCs insulted by OGD for 3 days compared with those under OGD treatment. When clemastine and OGD were added to 3-MA, the raise in PLP and VCAM1 expression levels was wakened, suggesting that clemastine alleviated hypomyelination by inhibiting the release of IL-1β via activation of autophagy. In summary, the molecular mechanisms by which clemastine improves axonal hypomyelination after ischemia–hypoxia are identified in the current study which may help in developing potential therapeutic strategies for axonal hypomyelination associated with HIBI.

Conclusion

This study determined that following ischemia–hypoxia challenge in rats, the activated astrocytes in the corpus callosum produced excess amounts of IL-1β. The ensuing cellular interaction between astrocytes and OPCs via IL-1β would impede the maturation of OPCs and lead to hypomyelination. Clemastine improved axonal hypomyelination by inhibiting neuroinflammation. Further analysis revealed that clemastine promoted the maturation of OPCs through inhibited the release of IL-1β by activation of autophagy in astrocytes. Further understanding of the process in which clemastine plays a key role in astrocyte activation will help to design effective treatment strategies to improve hypomyelination caused by HIBI.

Abbreviations

HIBI: Hypoxic-ischemic brain injury

OPCs: Oligodendrocyte progenitor cells

IL-1β: Interleukin-1beta

BCCAO: Bilateral common carotid artery occlusion

NLRP3: Nod-like receptor protein 3

HH1R: Histamine H1 receptor

OGD: Oxygen glucose deprivation

PBS: Phosphate-buffer saline

OPCDM: Oligodendrocyte precursor cell differentiation culture medium

FBS: Fetal bovine serum

PLP: Proteolipid protein

CNPase: 2′,3′-cyclic nucleotide-3′-phosphodiesterase

Declarations

Ethics approval and consent to participate

Approval of the Laboratory Animal Ethical and Welfare Committee Xin Hua Hospital Affiliated to Shanghai Jiao Tong University School of Medicine: XHEC-F-2018-038

Consent for publication

Not applicable

Availability of data and materials

The datasets used and analysed during the current study are available from the corresponding author on reasonable request.

Competing interests

The authors declare that they have no competing interests.

Funding

Grant sponsor: National Natural Science Foundation of China (Grant numbers: 81901930 and 81772111); Shanghai Health System Talents Training Program (Grant number: 2018BR13)

Authors' contributions

AHF. and SMP. conceived and designed the experiments. DX. and LN. performed the experiments. DX. and CJG. analyzed the data. AHF. and SMP. contributed reagents/materials/analysis tools. DX. wrote the article. XLG, YW, and YJZ participated in some animal experiments. All authors read and approved the final manuscript.

Acknowledgements

Not applicable.

Footnotes

* Correspondence: Email: Aihua Fei, feiaihua@xinhuamed.com.cn; Shuming Pan, panshuming@xinhuamed.com.cn.
Department of Emergency, Xinhua Hospital Affiliated to Shanghai Jiao Tong University School of Medicine, Yangpu District, Shanghai, China.

References

1. Sandroni C, D'Arrigo S, Nolan JP. Prognostication after cardiac arrest. Crit Care. 2018;22(1):150.
2. Santos PT, O'Brien CE, Chen MW, Hopkins CD, Adams S, Kulikowicz E, et al. Proteasome Biology Is Compromised in White Matter After Asphyxic Cardiac Arrest in Neonatal Piglets. J Am Heart Assoc. 2018;7(20):e009415.
3. Cronberg T. White matter is what matters after cardiac arrest. Lancet Neurol. 2018;17(4):291-292.
4. Xie D, Ge X, Ma Y, Tang J, Wang Y, Zhu Y, et al. Clemastine improves hypomyelination in rats with hypoxic-ischemic brain injury by reducing microglia-derived IL-1βvia P38 signaling pathway. J Neuroinflammation. 2020;17(1):57.
5. McDonald CA, Penny TR, Paton MCB, Sutherland AE, Nekkanti L, Yawno T, et al. Effects of umbilical cord blood cells, and subtypes, to reduce neuroinflammation following perinatal hypoxic-ischemic brain injury. J Neuroinflammation. 2018;15(1):47.
6. Tsuji S, Di Martino E, Mukai T, Tsuji S, Murakami T, Harris RA, et al. Aggravated brain injury after neonatal hypoxic ischemia in microglia-depleted mice. J Neuroinflammation. 2020;17(1):111.
7. Subedi L, Lee JH, Yumnam S, Ji E, Kim SY. Anti-Inflammatory Effect of Sulforaphane on LPS-Activated Microglia Potentially through JNK/AP-1/NF-κB Inhibition and Nrf2/HO-1 Activation. Cells. 2019;8(2). pii: E194.
8. Xie D, Shen F, He S, Chen M, Han Q, Fang M, et al. IL-1β Induces Hypomyelination in the Periventricular White Matter Through Inhibition of Oligodendrocyte Progenitor Cell Maturation via FYN/MEK/ERK Signaling Pathway in Septic Neonatal Rats. Glia. 2016;64(4):583-602.
9. Colombo E, Farina C. Astrocytes: Key Regulators of Neuroinflammation. Trends Immunol. 2016;37(9):608-620.
10. Garber C, Vasek MJ, Vollmer LL, Sun T, Jiang X, Klein RS. Astrocytes decrease adult neurogenesis during virus-induced memory dysfunction via IL-1. Nat Immunol. 2018;19(2):151-161.
11. Cho KS, Lee JH, Cho J, Cha GH, Song GJ. Autophagy Modulators and Neuroinflammation. Curr Med Chem. 2020;27(6):955-982.

12. Lotfi P, Tse DY, Di Ronza A, Seymour M, Martano G, Cooper JD, et al. Trehalose reduces retinal degeneration, neuroinflammation and storage burden caused by a lysosomal hydrolase deficiency. 2018;14(8):1419-1434.
13. Wang F, Ren SY, Chen JF, Liu K, Li RX, Li ZF, et al. Myelin degeneration and diminished myelin renewal contribute to age-related deficits in memory. Nat Neurosci. 2020;23(4):481-486.
14. Chen YM, He XZ, Wang SM, Xia Y. δ-Opioid Receptors, microRNAs, and Neuroinflammation in Cerebral Ischemia/Hypoxia. Front Immunol. 2020;11:421.
15. Zhang W, Smith C, Howlett C, Stanimirovic D. Inflammatory activation of human brain endothelial cells by hypoxic astrocytes in vitro is mediated by IL-1beta.J Cereb Blood Flow Metab. 2000;20(6):967-78.
16. Shiow LR, Favrais G, Schirmer L, Schang AL, Cipriani S, Andres C, et al. Reactive astrocyte COX2-PGE2 production inhibits oligodendrocyte maturation in neonatal white matter injury. Glia. 2017;65(12):2024-2037.
17. Malhotra S, Costa C, Eixarch H, Keller CW, Amman L, Martínez-Banaclocha H, et al. NLRP3 inflammasome as prognostic factor and therapeutic target in primary progressive multiple sclerosis patients. Brain. 2020. pii: awaa084.
18. He W, Long T, Pan Q, Zhang S, Zhang Y, Zhang D, et al. Microglial NLRP3 inflammasome activation mediates IL-1β release and contributes to central sensitization in a recurrent nitroglycerin-induced migraine model. J Neuroinflammation. 2019;16(1):78.
19. Uddin MS, Stachowiak A, Mamun AA, Tzvetkov NT, Takeda S, Atanasov AG, et al. Autophagy and Alzheimer's Disease: From Molecular Mechanisms to Therapeutic Implications.Front Aging Neurosci. 2018;10:04.
20. Ye J, Jiang Z, Chen X, Liu M, Li J, Liu N. The role of autophagy in pro-inflammatory responses of microglia activation via mitochondrial reactive oxygen species in vitro. J Neurochem. 2017;142(2):215-230.
21. Klionsky DJ, Abdelmohsen K, Abe A, Abedin MJ, Abeliovich H, Acevedo Arozena A, Adachi H, Adams CM, et al. Guidelines for the use and interpretation of assays for monitoring autophagy (3rd edition). Autophagy. 2016;12(1):1-222.
22. Sanjuan MA, Dillon CP, Tait SW, Moshiach S, Dorsey F, Connell S, et al. Toll-like receptor signalling in macrophages links the autophagy pathway to phagocytosis. Nature. 2007; 450:1253-7.
23. Bjørkøy G, Lamark T, Brech A, Outzen H, Perander M, Øvervatn A, et al. p62/SQSTM1 forms protein aggregates degraded by autophagy and has a protective effect on huntingtininduced cell death. J Cell Biol 2005; 171:603-14.
24. Luo SM, Ge ZJ, Wang ZW, Jiang ZZ, Wang ZB, Ouyang YC, et al. Unique insights into maternal mitochondrial inheritance in mice. Proc Natl Acad Sci USA 2013; 110:13038-43.
25. Bonfanti E, Gelosa P, Fumagalli M, Dimou L, Viganò F, Tremoli E, et al. The role of oligodendrocyte precursor cells expressing the GPR17 receptor in brain remodeling after stroke. Cell Death Dis. 2017;8(6):e2871.

26. Huang P, Zhou Q, Lin Q, Lin L, Wang H, Chen X1, et al. Complement C3a induces axonal hypomyelination in the periventricular white matter through activation of WNT/β-catenin signal pathway in septic neonatal rats experimentally induced by lipopolysaccharide. Brain Pathol. 2019 Oct 17. doi: 10.1111/bpa.12798.
27. Michalski D, Keck AL, Grosche J, Martens H, Härtig W. Immunosignals of Oligodendrocyte Markers and Myelin-Associated Proteins Are Critically Affected after Experimental Stroke in Wild-Type and Alzheimer Modeling Mice of Different Ages. Front Cell Neurosci. 2018;12:23.
28. Calabretta S, Vogel G, Yu Z, Choquet K, Darbelli L, Nicholson TB, et al. Loss of PRMT5 Promotes PDGFRα Degradation during Oligodendrocyte Differentiation and Myelination. Dev Cell. 2018;46(4):426-440.
29. Marie C, Clavairoly A, Frah M, Hmidan H, Yan J, Zhao C, et al. Oligodendrocyte precursor survival and differentiation requires chromatin remodeling by Chd7 and Chd8. Proc Natl Acad Sci U S A. 2018;115(35):E8246-E8255.
30. Miyamoto Y, Torii T, Tanoue A, Yamauchi J. VCAM1 acts in parallel with CD69 and is required for the initiation of oligodendrocyte myelination. Nat Commun. 2016;7:13478.
31. Flygt J, Ruscher K, Norberg A, Mir A, Gram H, Clausen F, et al. Neutralization of Interleukin-1β following Diffuse Traumatic Brain Injury in the Mouse Attenuates the Loss of Mature Oligodendrocytes. J Neurotrauma. 2018;35(23):2837-2849.
32. Zhou Y, Zhang J, Wang L, Chen Y, Wan Y, He Y, et al. Interleukin-1β impedes oligodendrocyte progenitor cell recruitment and white matter repair following chronic cerebral hypoperfusion. Brain Behav Immun. 2017;60:93-105.
33. Yang XL, Wang X, Shao L, Jiang GT, Min JW, Mei XY, et al. TRPV1 mediates astrocyte activation and interleukin-1β release induced by hypoxic ischemia (HI). J Neuroinflammation. 2019;16(1):114.
34. Wang XS, Yue J, Hu LN, Tian Z, Zhang K, Yang L, Zhang HN, et al. Activation of G protein-coupled receptor 30 protects neurons by regulating autophagy in astrocytes. Glia. 2020;68(1):27-43.
35. Huang R, Zhang Y, Han B, Bai Y, Zhou R, Gan G, et al. Circular RNA HIPK2 regulates astrocyte activation via cooperation of autophagy and ER stress by targeting MIR124-2HG. Autophagy. 2017;13(10):1722-1741.

Figures

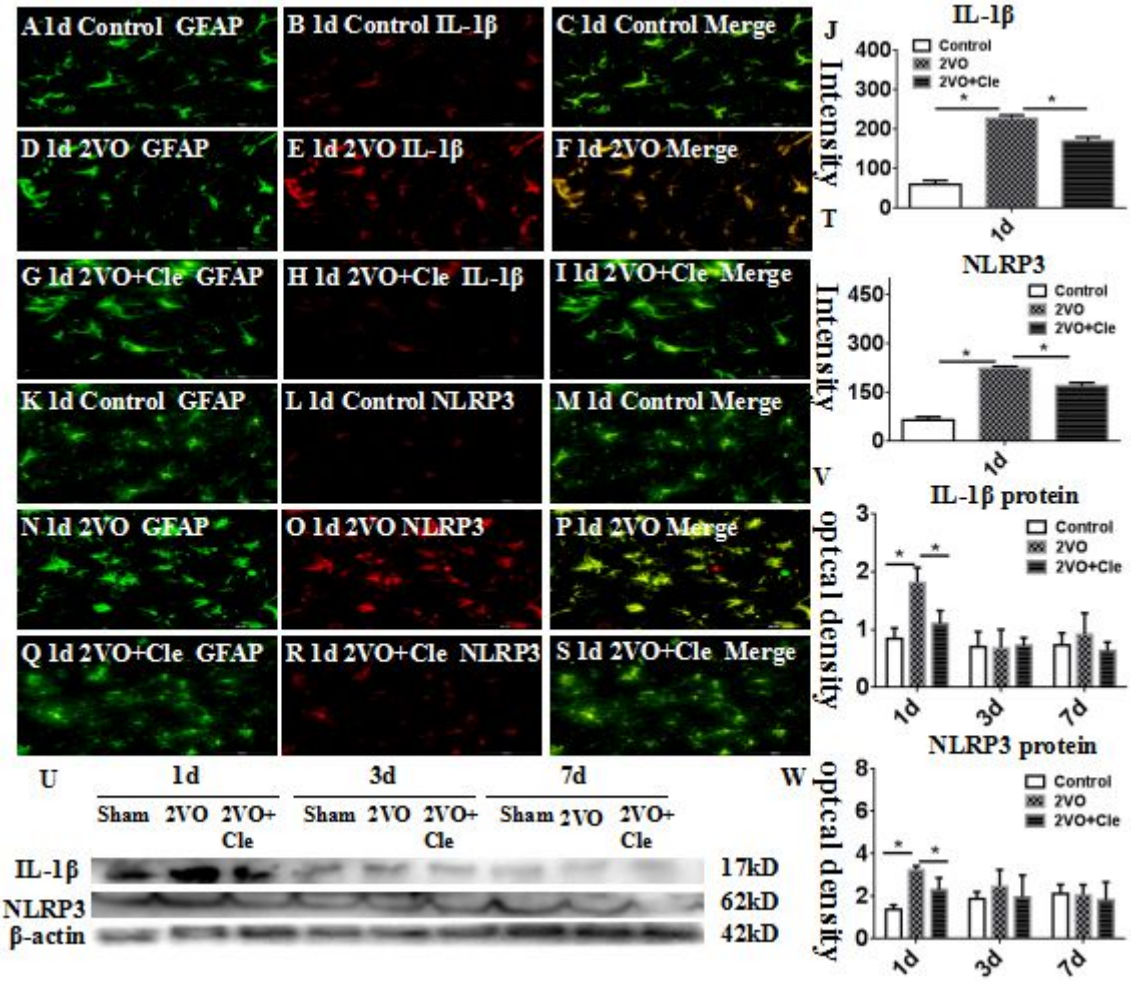

Figure 1

A–W show interleukin-1beta (IL-1β) and nod-like receptor protein 3 (NLRP3) protein expression levels in the corpus callosum of rats at 1, 3, and 7 days after the bilateral common carotid artery occlusion (BCCAO) and clemastine injection after BCCAO when compared with their corresponding controls. Double immunofluorescence staining showing the distribution of GFAP-labeled (A, D, G, K, N, and Q, green) and IL-1β (B, E, and H, red) and NLRP3 (L, O, and R, red) immunoreactive astrocytes in the corpus callosum of rats at 1day after BCCAO and clemastine injection after BCCAO and their corresponding controls. The colocalized expression of GFAP and IL-1β or NLRP3 in astrocytes can be seen in C, F, I, or M, P, S. Bar graphs (J and T) depict remarkable increased in the immunofluorescence intensity of IL-1β and NLRP3 expression levels, following BCCAO challenge when compared with matched controls; clemastine reversed these changes. Panel U shows IL-1β (17 kDa), NLRP3 (62 kDa), and β-actin (42 kDa) immunoreactive bands. Panels V and W show bar graphs depicting significant increases in the optical density of IL-1β and NLRP3 after BCCAO when compared with their corresponding controls. Meanwhile, clemastine could remarkably decrease the expression of IL-1β and NLRP3 at 1day. N = 3. *P < 0.05. Scale bars: A–S 50 μm.

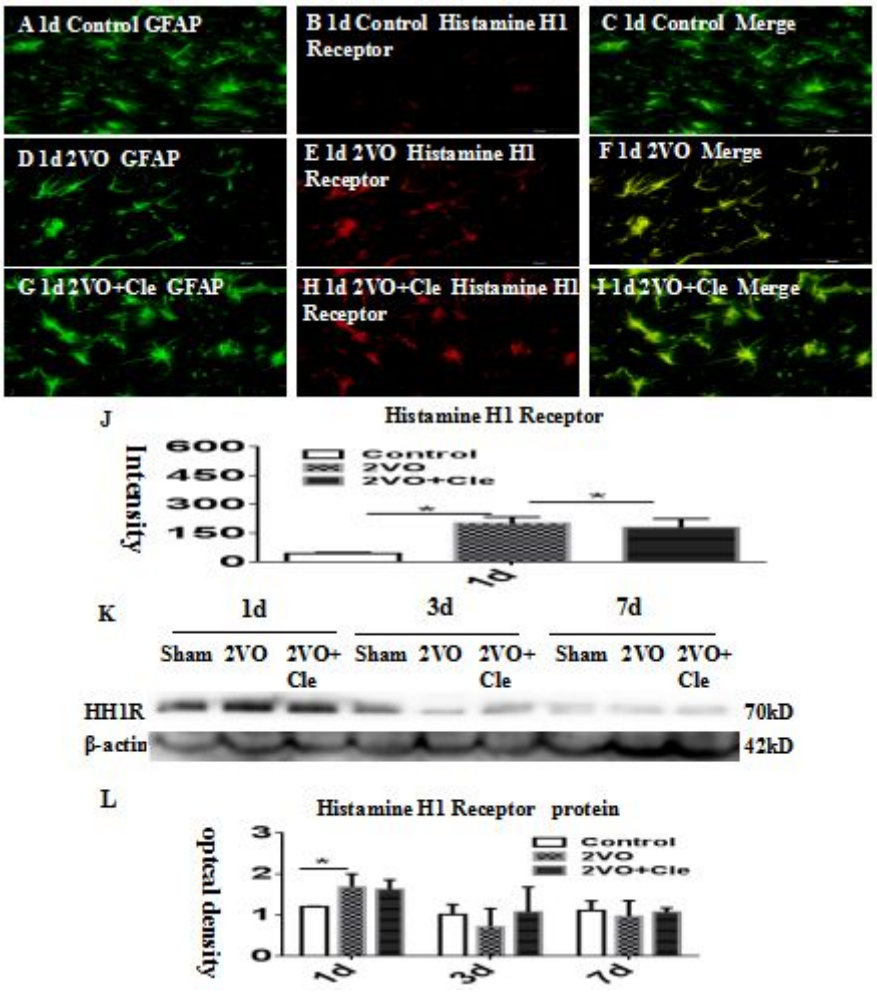

Figure 2

Histamine H1 receptor (HH1R) protein expression in the corpus callosum of rats at 1, 3, and 7 days after the bilateral common carotid artery occlusion (BCCAO) and clemastine injection after BCCAO when compared with their corresponding controls. Double immunofluorescence staining showing the distribution of GFAP-labeled (A, D, and G, green) and HH1R (B, E, and H, red) immunoreactive astrocytes in the corpus callosum of rats at 1 day after BCCAO and clemastine injection after BCCAO and their corresponding controls. The colocalized expression of GFAP and HH1R in astrocytes can be seen in C, F, and I. Panel J shows HH1R (70 kDa) and β-actin (42 kDa) immunoreactive bands. Panel K and L show bar graphs depicting significant increased in the immunofluorescence intensity and optical density of HH1R following the BCCAO when compared with their corresponding controls; clemastine showed no effect on the expression of HH1R. N = 3. *P < 0.05. Scale bars: A–I 50 μm.

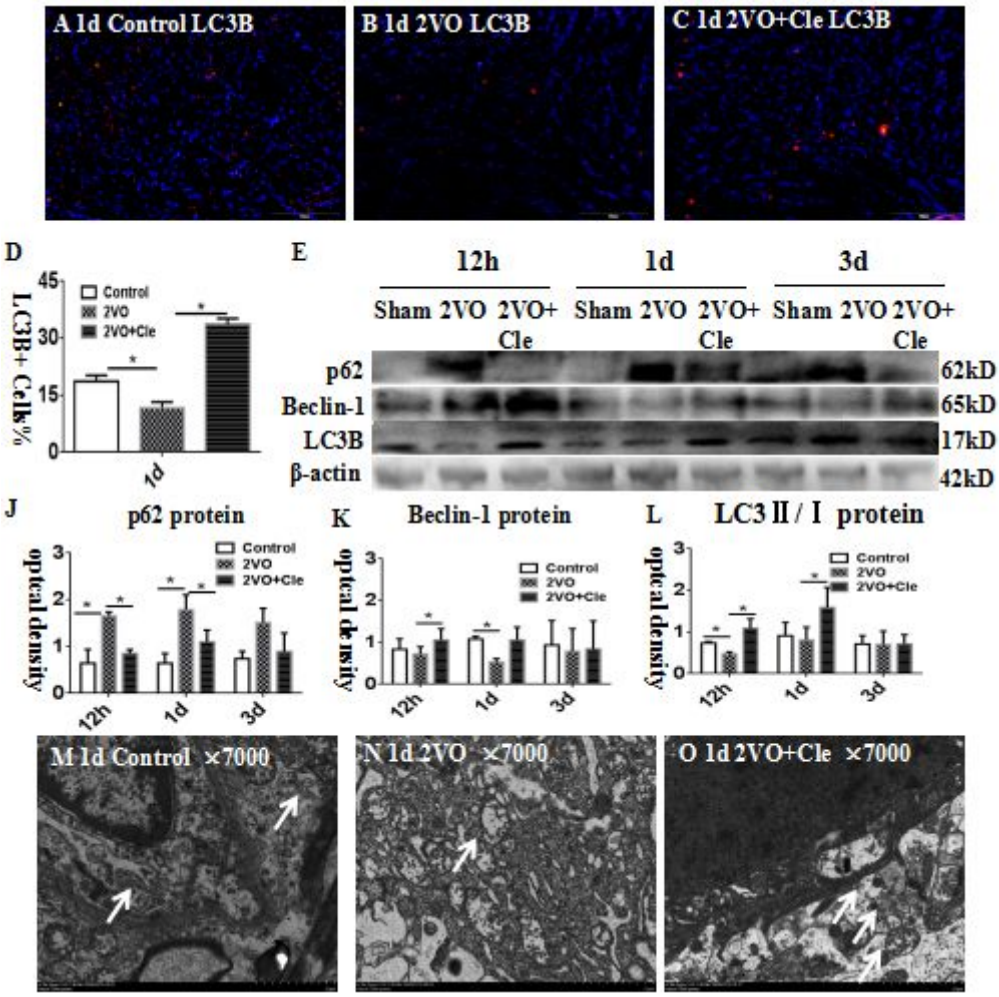

Figure 3

Immunofluorescence staining showing LC3B immunoreactive cells (red) in the corpus callosum of rats at 1 day after the bilateral common carotid artery occlusion and clemastine injection after BCCAO when compared with their corresponding controls (A-C). Bar graph in D shows a remarkable decrease in the corpus callosum at 1 day after the BCCAO when compared with their corresponding controls; clemastine could reverse this phenomenon. Panel E shows p62 (62 kDa), Beclin-1 (65 kDa), LC3B (17 kDa), and β-actin (42 kDa) immunoreactive bands. Panel J show bar graphs depicting significant decreases in the optical density of p62 at 0.5, 1, and 3 days following the BCCAO when compared with their corresponding controls; clemastine downregulated the expression of p62. Panel K and L show bar graphs depicting a significant decrease in the optical density of Beclin-1 and LC3B at 1 day following the BCCAO when compared with their corresponding controls;Beclin-1 and LC3B protein increases significantly at 1 day after treatment with clemastine compared with that of BCCAO.Transmission electron microscopy of brain revealed that astrocytes after BCCAO presented less cytoplasmic vacuolization than that in contro at l day. The vacuoles were filled with amorphous or electron-dense material and were surrounded by a single or a double membrane (M and N). clemastine could reverse this phenomenon (O). N = 3. *P < 0.05. Scale bars: A–C 200 μm. EM:2μm.

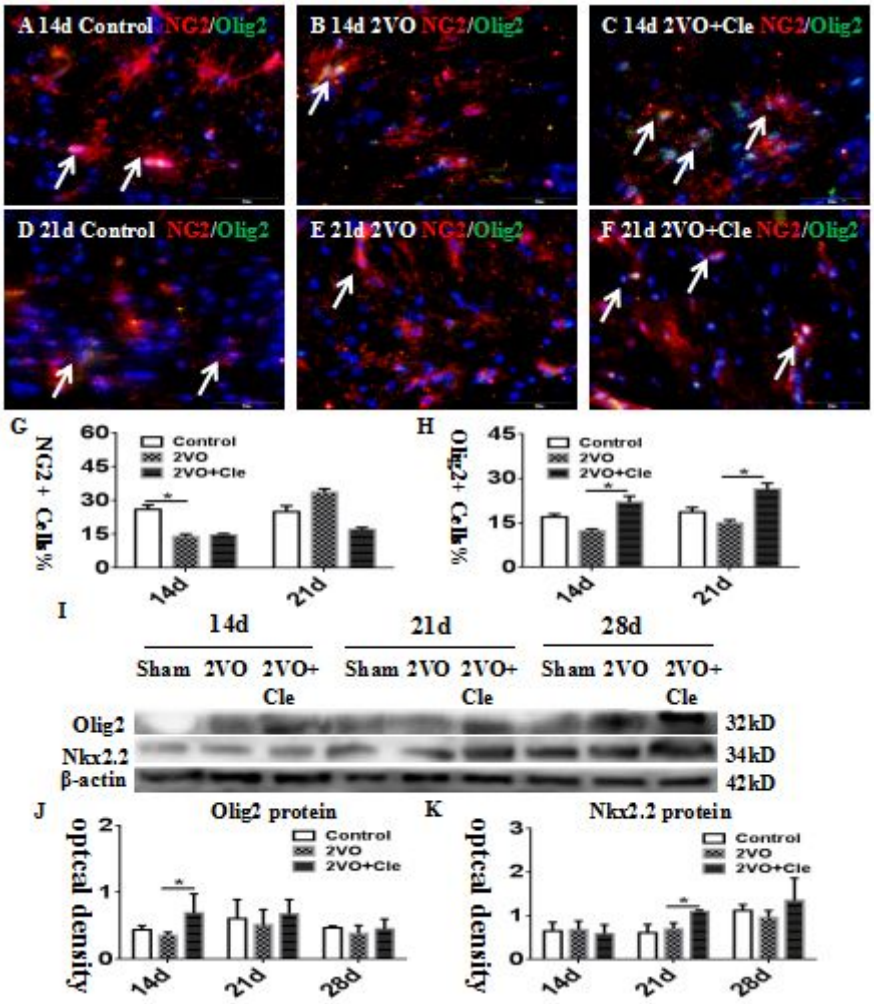

Figure 4

Immunofluorescence staining showing NG2 and Olig2 immunoreactive oligodendrocytes (NG2, red; Olig2, green) in the corpus callosum of rats at 14, 21 days after the BCCAO (B, E) and clemastine injection after BCCAO (C, F) when compared with their corresponding controls (A, D). Bar graph in G shows a significant decrease in the cell number of NG2-positive oligodendrocytes/mm2 in the corpus callosum at 14d after the BCCAO model and clemastine injection when compared with their corresponding controls. Bar graph in H shows a significant decrease in the cell number of Olig2-positive oligodendrocytes/mm2 in the corpus callosum at 14, 21d after the BCCAO model when compared with their corresponding controls, clemastine could reverse this phenomenon. Panel I shows Olig2 (32 kDa), Nkx2.2 (34 kDa), and β-actin (42 kDa) immunoreactive bands. Panel J and K show bar graph depicting significant changes in the optical density of Nkx2.2 and Olig2 following the clemastine injection when compared with BCCAO model and their corresponding controls. The Olig2 protein levels in the corpus callosum at 14 d and Nkx2.2 at 21d after the BCCAO are significantly decrease when compared with clemastine injection. *P < 0.05. Scale bars: A–F 50μm.

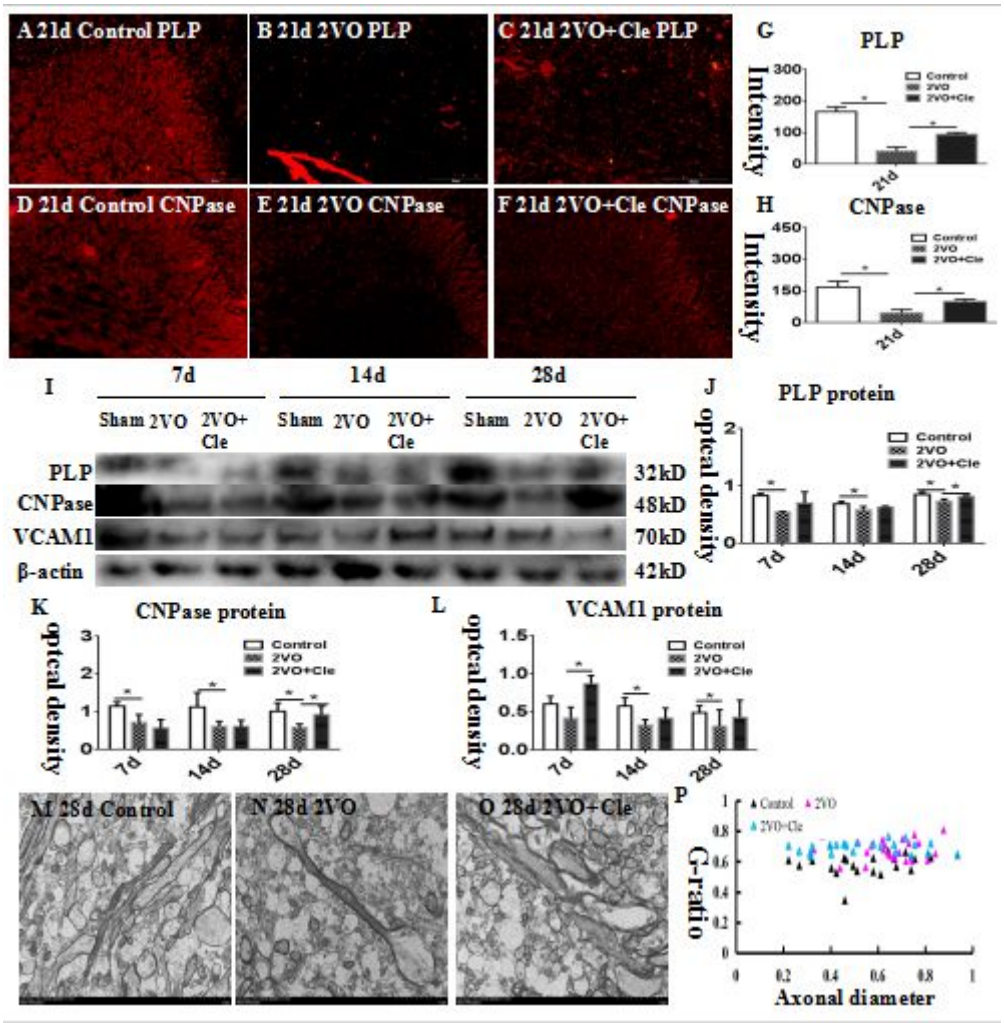

Figure 5

Hypomyelination in the corpus callosum of rats at 21 day after the bilateral common carotid artery occlusion (BCCAO; A–F). Immunofluorescence staining showing proteolipid protein (PLP) and 2′,3′-cyclic nucleotide-3′-phosphodiesterase (CNPase) expression in the corpus callosum of rats at 21 days after the BCCAO (B and E) and clemastine injection after BCCAO (C and F) and their corresponding controls (A and D). Bar graph in G and H shows a significant decrease in the immunofluorescence intensity of PLP and CNPase in the corpus callosum at 21 days after the BCCAO when compared with their corresponding controls; clemastine reversed these changes. Panel I shows PLP (32 kDa), CNPase (48 kDa), VCAM1(70 kDa) and β-actin (42 kDa) immunoreactive bands. Panels J, K and L show bar graphs depicting significant decreases in the optical density of PLP, CNPase and VCAM1 at 7, 14, and 28 days following the BCCAO when compared with their corresponding controls; clemastine reversed these changes at 28 days (*P < 0.05; J–L) Electron micrographs showing hypomyelination and aberrant ensheathment of axons in the corpus callosum at 28 days after the BCCAO. The number of myelinated axons in the corpus callosum of 28-day rats in BCCAO group (N) decreases remarkably when compared with their corresponding controls (M), treated with clemastine which could reverse the hypomyelination after the BCCAO (O). (P) Scatter plots of g-ratios against axon diameters in the corpus callosum at 28 days are shown. G-ratios increased after BCCAO when compared with their corresponding controls; clemastine

reversed the changes, indicating that clemastine could promote myelin formation in the myelinated fibers. N = 3. Scale bars: A–F, 200 μm; J-L, 10 μm.

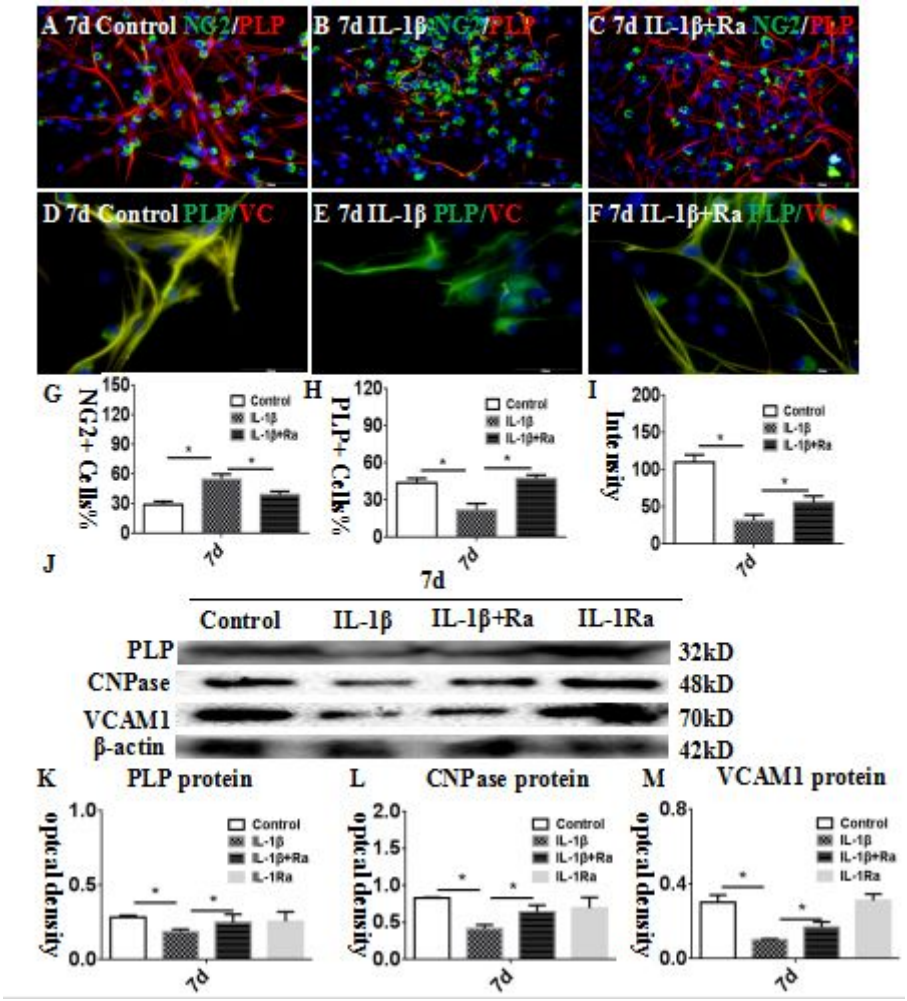

Figure 6

IL-1β inhibits differentiation of oligodendrocyte progenitor cells (OPCs) in vitro. Immunofluorescence images of cultured OPCs show the ratios of NG2 (A–C, green) and PLP (A–C, red) at 7 days after IL-1β administration (B) or IL-1β + IL-1Ra treatment (C) when compared with their corresponding controls (A). Bar graph in G and H shows a remarkable increase in the ratio of NG2-positive oligodendrocytes and decrease in the ratio of PLP-positive oligodendrocytes at 7 days after IL-1β administration when compared with their corresponding controls; IL-1Ra reversed these changes. Immunofluorescence images of cultured OPCs show the co-location of PLP and VCAM1 (D–F, yellow) at 7 days. Bar graph in I shows a remarkable decrease in the expression of VCAM1 at 7 days after IL-1β administration when compared with their corresponding controls; IL-1Ra reversed these changes. Panel J shows PLP (32 kDa), CNPase (48 kDa),VCAM1(70 kDa) and β-actin (42 kDa) immunoreactive bands. Bar graphs in K, L and M show significant decreases in the optical density of PLP, VCAM1 and CNPase at 7 days after IL-1β administration when compared with their corresponding controls. The IL-1Ra may attenuate the status. N = 3. *P < 0.05. Scale bars: A–F 50 μm.

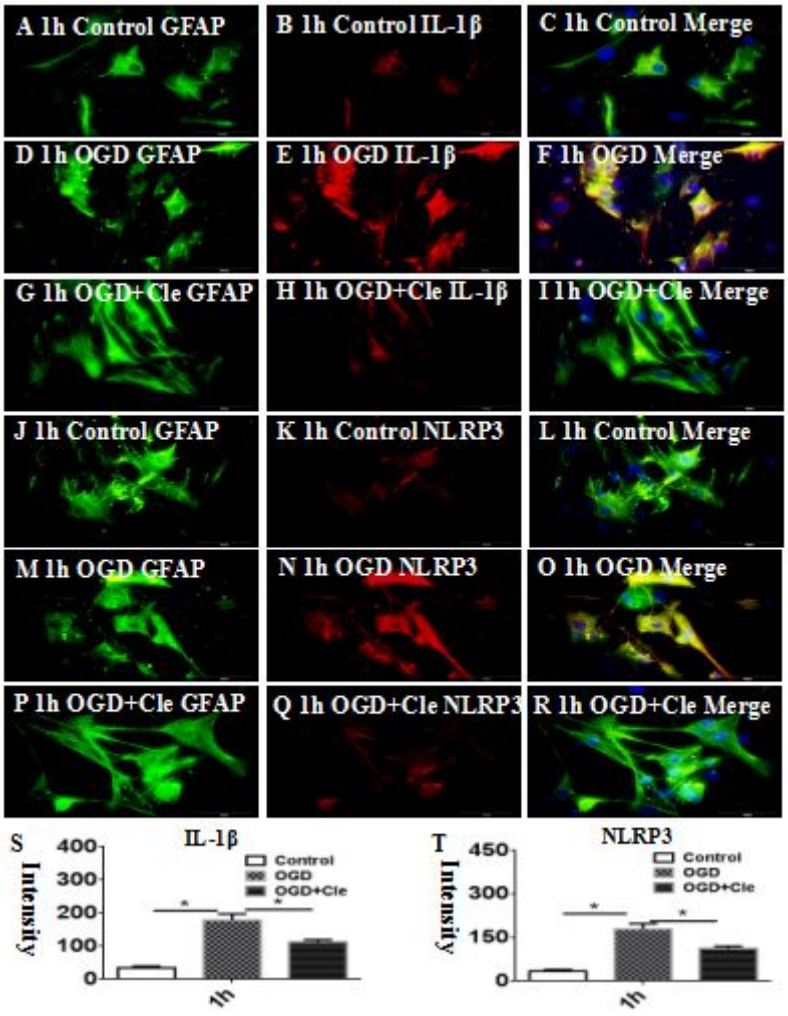

Figure 7

Clemastine inhibits expression of IL-1β and NLRP3 protein of astrocytes insulted by oxygen glucose deprivation (OGD) in vitro. Double immunofluorescence staining showing the distribution of GFAP-labeled (A, D, G, J, M, and P, green) and IL-1β (B, E, and H, red) and NLRP3 (K, N, and Q, red) immunoreactive astrocytes in vitro at 1 h after OGD and OGD+clemastine and their corresponding controls. The colocalized expression of GFAP and IL-1β or NLRP3 in astrocytes can be seen in C, F, I, or L, O, R, respectively. Bar graphs (S and T) depicting significant increase in the immunofluorescence intensity of IL-1β and NLRP3 expression, respectively, following OGD challenge when compared with matched controls, clemastine reversed these changes. N=3. *P < 0.05. Scale bars: A–R 50μm.

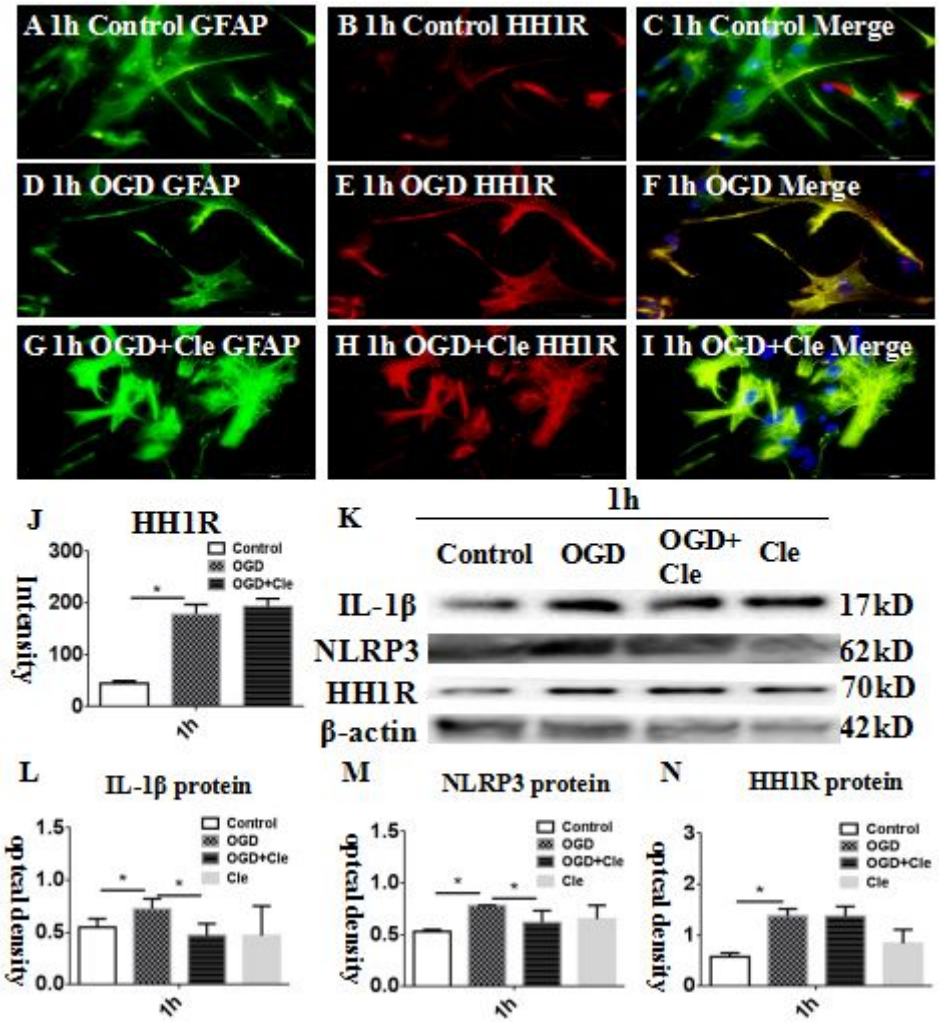

Figure 8

Clemastine inhibits expression of IL-1β and NLRP3 and exerts no effect on the expression of HH1R of astrocytes in vitro. Double immunofluorescence staining showing the distribution of GFAP-labeled (A, D and G, green) and HH1R (B, E and H, red) immunoreactive astrocytes in vitro at 1 h after OGD and OGD + clemastine and their corresponding controls. The colocalized expression of GFAP and HH1R in astrocytes can be seen in C, F, and I. Panel J and N show bar graphs depicting significant increases in the immunofluorescence intensity and optical density of HH1R following the OGD when compared with their corresponding controls, clemastine showed no effect on the expression of HH1R. Panel K showing IL-1β (17 kDa), NLRP3 (62 kDa), HH1R (70 kDa), and β-actin (42 kDa) immunoreactive bands. Panels L and M are bar graphs which indicate that expression of IL-1β and NLRP3 were improved in the astrocytes after OGD administration for 1h. The clemastine may attenuate the increment. N=3. *P < 0.05. Scale bars: A–I 50μm.

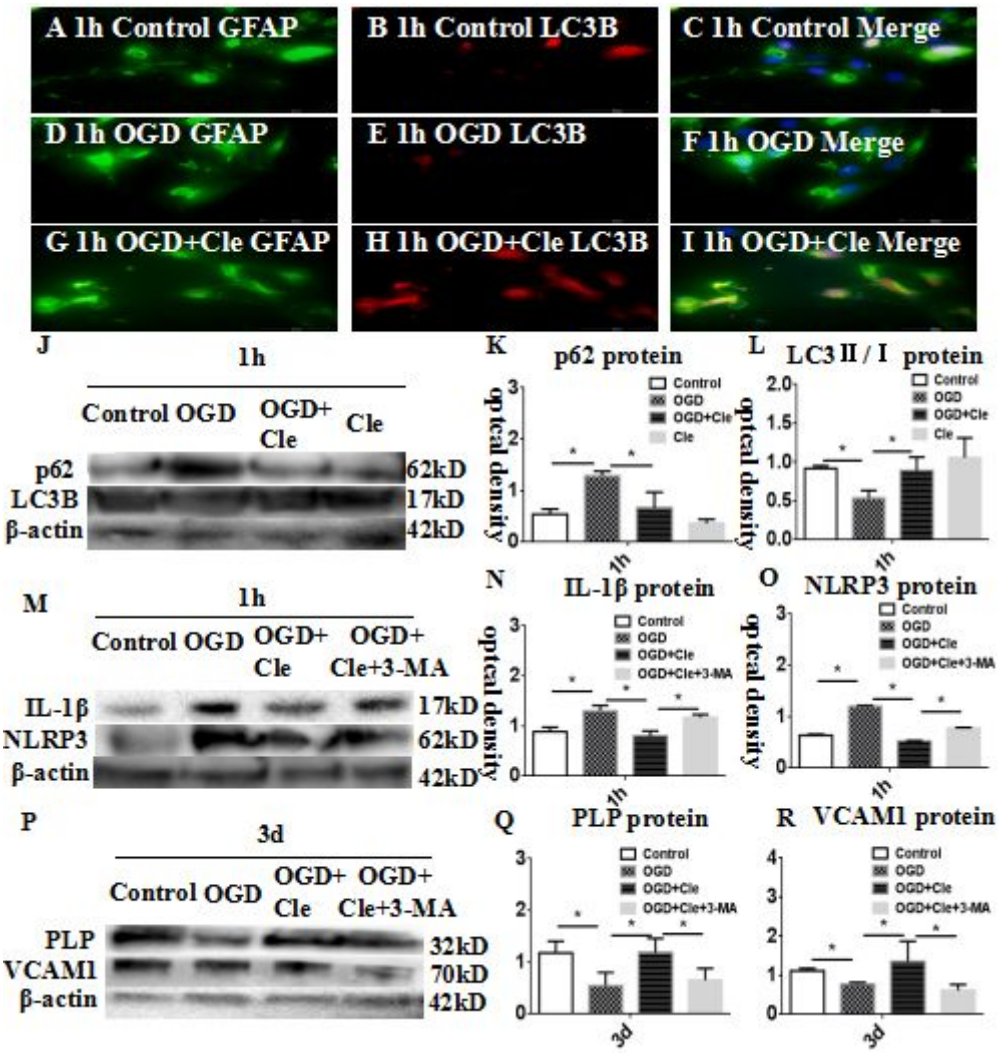

Figure 9

Clemastine improves axonal hypomyelination via activation of autophagy in astrocytes. Double immunofluorescence staining showing the distribution of GFAP-labeled (A, D and G, green) and LC3B (B, E and H, red) immunoreactive astrocytes in vitro at 1 h after OGD and OGD + clemastine and their corresponding controls. The colocalized expression of GFAP and LC3B in astrocytes can be seen in C, F, and I. Panel J showing p62 (62 kDa) and LC3B (17 kDa) immunoreactive bands. Panel K is bar graph which indicate that expression of p62 increase in astrocytes after OGD administration for 1 h. The clemastine may attenuate the increment. Panel L is bar graph showing the expression of LC3Ba was significantly down-regulated at 1 h after treatment with OGD compared with the controls. Clemastine could improve the expressions of LC3B. Panel M showing IL-1β (17 kDa), NLRP3 (62 kDa), and β-actin (42 kDa) immunoreactive bands. Panel P showing PLP (32 kDa), VCAM1 (70 kDa), and β-actin (42 kDa) immunoreactive bands. Panel N and O are bar graphs showing the protein expressions of IL-1β and NLRP3 were significantly up-regulated at 1 h after OGD compared with the controls. Clemastine could downregulate the expressions of IL-1β and NLRP3 proteins induced by OGD. When additional 3-MA was added, the effect is weakened. Panel Q and R are bar graphs showing the protein expressions of PLP and

VCAM1 were significantly down-regulated at 1 h after OGD compared with the controls. The effect of clemastine on PLP and VCAM1 were antagonized by 3-MA. N=3. *P < 0.05.